

Quantum critical behavior in heavy electron materials

 Yi-feng Yang^{a,b,1} and David Pines^{c,1}
^aBeijing National Laboratory for Condensed Matter Physics and Institute of Physics, Chinese Academy of Sciences, Beijing 100190, China; ^bCollaborative Innovation Center of Quantum Matter, Beijing 100190, China; and ^cSanta Fe Institute and Department of Physics, University of California, Davis, CA 95616

Contributed by David Pines, April 29, 2014 (sent for review March 26, 2014; reviewed by Gilbert George Lonzarich and Zachary Fisk)

Quantum critical behavior in heavy electron materials is typically brought about by changes in pressure or magnetic field. In this paper, we develop a simple unified model for the combined influence of pressure and magnetic field on the effectiveness of the hybridization that plays a central role in the two-fluid description of heavy electron emergence. We show that it leads to quantum critical and delocalization lines that accord well with those measured for CeCoIn₅, yields a quantitative explanation of the field and pressure-induced changes in antiferromagnetic ordering and quantum critical behavior measured for YbRh₂Si₂, and provides a valuable framework for describing the role of magnetic fields in bringing about quantum critical behavior in other heavy electron materials.

heavy fermion | quantum criticality | two-fluid model

One of the most striking examples of emergent behavior in quantum matter is the emergence of the itinerant heavy electron liquid in materials that contain a Kondo lattice of localized f electrons coupled to background conduction electrons. Although we do not yet have a microscopic picture of heavy electron emergence and subsequent behavior, a phenomenological two-fluid model has been shown to provide a quantitative description of the way in which the collective hybridization of the localized f electron spin liquid (SL) with the background conduction electrons in a Kondo lattice gives rise to a new state of matter, the Kondo liquid (KL) heavy electron state, that coexists with a SL of partially hybridized local moments over much of the phase diagram (1–7). One can, for example, decompose the static spin susceptibility or spin–lattice relaxation rate into KL and hybridized SL components, e.g.,

$$\chi(T, p) = f(T, p)\chi_{KL}(T, p) + [1 - f(T, p)]\chi_{SL}(T, p), \quad [1]$$

where the strength of the KL component is measured by (1)

$$f(T, p) = \min \left\{ f_0(p) \left(1 - \frac{T}{T^*} \right)^{3/2}, 1 \right\}. \quad [2]$$

T^* , the coherence temperature at which the KL emerges (2), sets the energy scale for its subsequent universal behavior (3–5), brought about by the collective hybridization, and $f_0(p)$ measures its effectiveness (1).

The two-fluid model enables one to follow in detail the emergent behavior of both the KL and the residual hybridized local moments. The point at which $f(T, p) = 1$ is special, as it marks a delocalization phase transition from partially localized to fully itinerant heavy electron behavior. When the hybridization effectiveness parameter $f_0 = 1$, that phase transition occurs at absolute zero temperature, and represents a quantum critical point (QCP) that gives rise to unusual quantum critical behavior in the itinerant heavy electrons that is sometimes observed up to comparatively high temperatures (8, 9). Quite generally, if $f_0 < 1$, the hybridized SL becomes antiferromagnetically ordered, whereas the coexisting KL may become superconducting. On the other hand, if $f_0 > 1$, the delocalization phase transition will occur along a line of quantum criticality that is determined by T^* and the strength of the

hybridization effectiveness, and, in the two-fluid model, is given by

$$T_L(p) = T^*(p) \left[1 - f_0(p)^{-2/3} \right]. \quad [3]$$

 Below T_L , collective hybridization is complete, $f = 1$, and one encounters only itinerant heavy electron behavior.

Importantly, it is found experimentally that both the QCP and the delocalization line, T_L , can be shifted by applying an external magnetic field. One finds field-induced quantum criticality, such as has been observed in YbRh₂Si₂ (10), or a quantum critical line on the pressure–magnetic field phase diagram, as has been observed in CeCoIn₅ (11, 12). These results raise the question of whether such behavior can be described within the framework of the two-fluid model, and whether that model can provide physical insight into the origin of these changes. We show in the present paper that the answer to both questions is “yes”—that by taking into account the influence of external magnetic fields on the hybridization effectiveness parameter, f_0 , we can obtain a quantitative understanding of field-induced quantum criticality within a simple framework that provides some unexpected connections between the manifestations of that behavior. Moreover, because experiment shows that T^* is not changed by external magnetic fields (13), it is highly likely that the field-induced changes in the hybridization effectiveness parameter, $f_0(p, H)$, that we find explains the new delocalization line, $T_L(p, H)$, and a number of other emergent quantum critical phenomena, are not of collective origin, but must instead originate in field-induced single-ion Kondo local moment hybridization.

A Two-Fluid Description of the Influence of Magnetic Fields on Hybridization Effectiveness, Quantum Criticality, Delocalization, and Other Physical Phenomena

 We begin by writing the field-induced changes in f_0 as

Significance

Quantum critical behavior occurs when a material is near a zero temperature phase transition between two ordered forms of matter. Kondo lattice materials, in which itinerant heavy (~200 bare mass) electrons emerge through the collective hybridization of localized f electrons with background conduction electrons, provide a rich source of experimental information about how, for example, pressure and magnetic fields influence local moment antiferromagnetic order and its boundary with competing fully itinerant heavy electron behavior in the pressure–magnetic field plane. A phenomenological two-fluid model of coupled local moments and itinerant heavy electrons enables us to calculate both and obtain a quantitative account of related quantum critical behavior in two of the best-studied heavy electron materials, CeCoIn₅ and YbRh₂Si₂.

Author contributions: Y.-f.Y. and D.P. designed research; Y.-f.Y. and D.P. performed research; Y.-f.Y. analyzed data; and Y.-f.Y. and D.P. wrote the paper.

Reviewers: G.G.L., University of Cambridge; and Z.F., University of California, Irvine.

The authors declare no conflict of interest.

¹To whom correspondence may be addressed. E-mail: yifeng@iphy.ac.cn or david.pines@gmail.com.

$$f_0(p, H) = f_0(p) [1 + (\eta_H H)^\alpha], \quad [4]$$

where we introduce a scaling parameter α to allow for the possibility that quantum criticality can lead to scaling behavior in the local hybridization effectiveness. Both α and η_H are assumed to be independent of pressure and to not change across the QCP, and magnetic field effects are considered only to the lowest order in H^α . Although the above scaling formula may only be valid in the quantum critical regime and a cross-over to a different form may take place at higher temperatures where collective hybridization dominates, we assume, for simplicity, the validity of Eqs. 3 and 4 in the whole parameter range and explore their consequences.

In the vicinity of the QCP, we may expand $f_0(p)$ as

$$f_0(p) \approx 1 + \eta_p (p - p_c^0), \quad [5]$$

where p_c^0 is the quantum critical pressure at $H = 0$, η_p is a constant, and we are assuming that all pressure-induced changes in f_0 are of collective origin so that quantum criticality does not bring about any power-law dependence in $(p - p_c^0)$. In general, we shall see that for Ce compounds, collective hybridization is enhanced with increasing pressure so that $\eta_p > 0$, whereas for Yb compounds, collective hybridization is suppressed with increasing pressure and $\eta_p < 0$. For both compounds, we are assuming that local hybridization is enhanced by the magnetic field and that the pressure-induced enhancement/suppression does not change at the QCP although such a change is in principle possible and may take place in CeRhIn₅ (1).

At the field-induced QCP, $f_0(p, H) = 1$, and Eq. 4 yields a simple relationship between f_0 and the quantum critical field H_{QC} ; at ambient pressure, we have

$$f_0 = \left(1 + \eta_H^\alpha H_{QC}^\alpha\right)^{-1}. \quad [6]$$

It follows directly that the delocalization line at ambient pressure depends in a simple way on T^* , H_{QC} , and η_H :

$$\frac{T_L(H)}{T^*} = 1 - \left(\frac{1 + \eta_H^\alpha H_{QC}^\alpha}{1 + \eta_H^\alpha H^\alpha}\right)^{2/3}. \quad [7]$$

At zero temperature, $f_0(p, H) = 1$ predicts a line of QCPs on the pressure–magnetic field plane; on combining Eq. 4 and [5], we obtain the field dependence of the quantum critical pressure,

$$p_c(H) = p_c^0 - \frac{1}{\eta_p} \frac{\eta_H^\alpha H^\alpha}{1 + \eta_H^\alpha H^\alpha}, \quad [8]$$

which for sufficiently large fields saturates at

$$p_c^\infty = p_c^0 - \eta_p^{-1}. \quad [9]$$

η_p^{-1} is seen to measure the difference between the high magnetic field and zero magnetic field quantum critical pressures. At the critical field, H_{QC} , at ambient pressure, Eq. 8 gives

$$\eta_p = \frac{1}{p_c^0} \frac{\eta_H^\alpha H_{QC}^\alpha}{1 + \eta_H^\alpha H_{QC}^\alpha}, \quad [10]$$

and the quantum critical line may be rewritten as

$$\frac{p_c(H)}{p_c^0} = 1 - \frac{1 + \eta_H^\alpha H_{QC}^\alpha}{1 + \eta_H^\alpha H^\alpha} \left(\frac{H}{H_{QC}}\right)^\alpha. \quad [11]$$

Eqs. 7 and 11 provide a key connection between scaling behavior, the quantum critical line on the p – H phase diagram, and the field

dependence of the delocalization line at ambient pressure that can easily be tested experimentally.

We note there are a number of candidate experimental signatures of T_L : First, because a change in the heavy electron Fermi surface is expected at T_L , density fluctuations associated with that change may lead to a maximum in the magnetoresistivity, as is seen in CeCoIn₅ (12); second, because below T_L one has only the itinerant heavy electrons present, the Knight shift will once more track the magnetic susceptibility, as is observed in URu₂Si₂ (14); a third signature may be a rapid cross-over in the Hall coefficient at T_L , as is observed in YbRh₂Si₂ (15); and a fourth may be inferred from the measurements of the contribution to the spin–lattice relaxation rate from the “hidden” heavy electron quantum critical spin fluctuations, as discussed in detail below.

The influence of magnetic fields on other physical quantities of interest is easily calculated using the above model and provides further tests of its usefulness. For example, because the Néel temperature, at which long range local moment order appears when $f(p, H) < 1$, is roughly proportional to the strength of the SL component at T_N , its field dependence is given by

$$\frac{T_N(p, H)}{T_N^0} = 1 - f(T_N, p, H), \quad [12]$$

where T_N^0 is the hypothetical antiferromagnetic ordering temperature of the f -electron lattice in the absence of any hybridization (1). In the two-fluid model, both T_N^0 and T^* are determined by the local moment interaction (2), so we have $T_N^0 = \eta_N T^*$, where η_N is a constant prefactor determined by frustration effects.

In a second example, the specific heat coefficient in the Fermi liquid state acquires a magnetic field dependence through $T_L(H)$. In the KL state, it displays a mild logarithmic divergence (1),

$$\gamma_{KL}(H) \approx \frac{S_{KL}(H)}{T_L(H)} = \frac{R \ln 2}{2T^*} \left[2 + \ln \frac{T^*}{T_L(H)}\right], \quad [13]$$

where R is the gas constant. However, in the vicinity of the quantum critical line that marks the end of localized behavior, experiment shows that quantum critical fluctuations give rise to a power-law scaling behavior that strongly enhances the effective mass. We take these into account with a simple scaling expression,

$$\frac{m^*}{m_0} = \left(\frac{T^*}{T_L(H)}\right)^{\alpha/2}, \quad [14]$$

in which $T_L(H)$ marks the distance to the QCP, the scaling exponent, $\alpha/2$, has been chosen by our fit to the experimental data for CeCoIn₅ and YbRh₂Si₂, and m_0 is a bare reference electron mass. The total specific heat coefficient is then given by

$$\gamma_{QC}(H) = \gamma_0 \left(\frac{T^*}{T_L(H)}\right)^{\alpha/2}, \quad [15]$$

where γ_0 is independent of the magnetic field. The appearance of the same scaling exponent, α , in Eqs. 4 and 14 suggests that both have a local origin.

A third quantity of interest is the magnetoresistivity, which in the Fermi liquid regime is given by $\rho(T, H) = A(H)T^2$. If we assume that the Kadowaki–Woods ratio, $A(H)/\gamma(H)^2$, is constant, Eq. 15 leads to another testable prediction of our model,

$$A(H) = \frac{A_0}{(T^*)^2} \left(\frac{T^*}{T_L(H)}\right)^\alpha, \quad [16]$$

where A_0 is the field-independent prefactor.

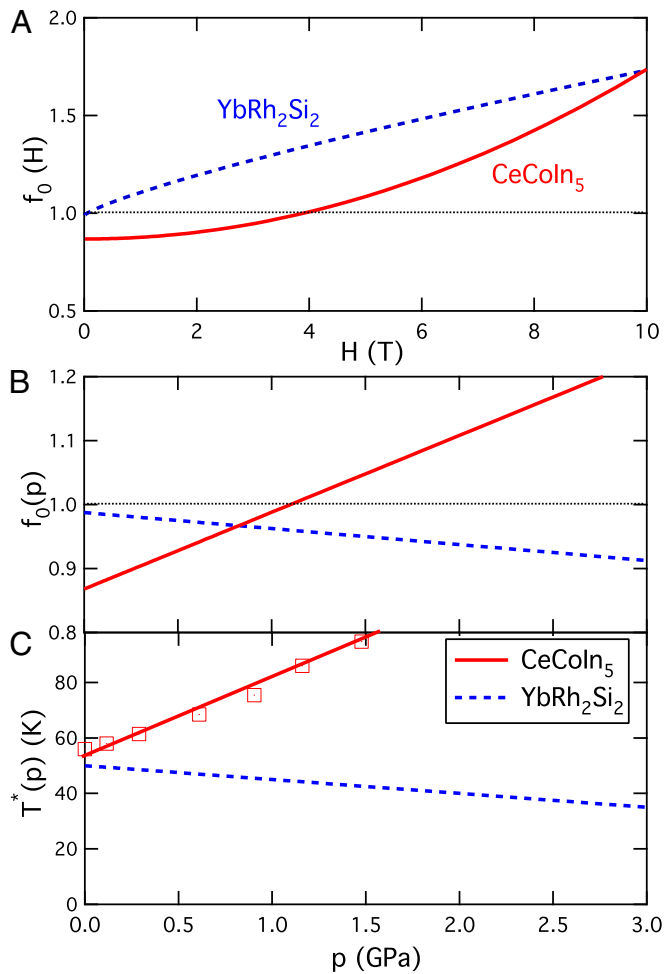


Fig. 3. Field and pressure dependence of the hybridization parameter, f_0 , and T^* for CeCoIn_5 and YbRh_2Si_2 . (A) Field dependence of f_0 at ambient pressure. (B) Pressure dependence of f_0 at zero field. (C) Pressure dependence of T^* at zero field (16).

resonance (NQR) spin–lattice relaxation rate (21) shown in Fig. 2B takes the form

$$\frac{1}{T_1} = \frac{1-f(T,p,H)}{T_1^{SL}} + \frac{f(T,p,H)}{T_1^{KL}}, \quad [17]$$

where T_1^{SL} and T_1^{KL} are the intrinsic spin–lattice relaxation time of the hybridized local moment SL and the itinerant KL, respectively. On assuming that the linear temperature dependence of the local moment $1/T_1^{SL}$ measured above T^* continues down to T_c , and making use of our new results for $f_0(p)$, we obtain the local moment contribution to $1/T_1$ shown by the dotted lines in Fig. 2B, and find that the KL relaxation time takes the simple form,

$$T_1^{KL} T \propto [T + T_x(p)], \quad [18]$$

where the pressure-dependent offset takes the values shown in Fig. 2B, *Inset*. These results suggest that there may be a second QCP in CeCoIn_5 , one that marks the end of local moment antiferromagnetic order, located at the point where the extrapolation of $T_x(p)$ to negative pressure goes to zero, ~ -0.5 GPa.

From Eq. 2, we find that at the superconducting transition temperature, $T_c = 2.2$ K, the KL hybridization parameter is $f(T_c) \approx 0.82$, suggesting that at zero field, almost 20% of the hybridized localized f moments are still present when the

material becomes superconducting. This is in agreement with the well-known observation of the magnetic susceptibility that shows a modified Curie–Weiss behavior above T_c with a reduced moment of about 10% (3). Our finding raises the interesting question of the role played by these localized magnetic moments in determining T_c and the properties of the superconducting state.

YbRh_2Si_2

YbRh_2Si_2 is of interest because it belongs to a well-studied non-Ce-based family that displays a wide variety—and at first sight, conflicting—signatures of quantum critical behavior (22–30).

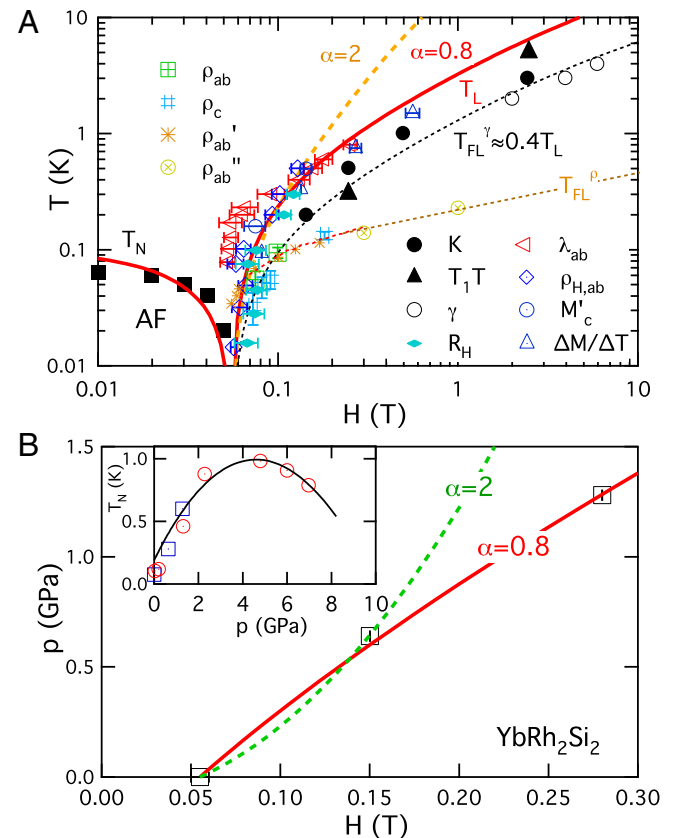


Fig. 4. The field-dependent Néel temperature, delocalization line, and quantum critical line of YbRh_2Si_2 . (A) A comparison of our proposed field-dependent Néel temperature T_N and delocalization line T_L with the experimental results for delocalization temperatures and the Landau Fermi liquid cross-over line obtained by different groups. (i) The delocalization temperature scales determined from the magnetostriction, λ , with $H_{QC} = 0.05$ T; magnetization, $M' = M + H(\partial M/\partial H)$, for a field perpendicular to the c axis and $H_{QC} = 0.06$ T; the Hall resistivity, ρ_H , for a field along the c axis ($H_{QC} = 0.066$ T, scaled by a factor of 13.2); and the Landau Fermi liquid cross-over determined from the resistivity, ρ_{ab}' , with $H_{QC} = 0.05$ T (22). (ii) The cross-over in the Hall coefficient with $H_{QC} = 0.06$ T (15). (iii) Maxima in $-(\Delta M/\Delta T)$ (26). (iv) The Fermi liquid cross-over determined by the temperature at which the Knight shift, K , the spin–lattice relaxation time, $T_1 T$, and the specific heat γ become constant ($H_{QC} = 0.05$ T) (10). (v) The Fermi liquid cross-over determined from resistivity, ρ_{ab} , ρ_{ab}'' ($H_{QC} = 0.06$ T) and ρ_c ($H_{QC} = 0.66$ T, scaled by a factor of 11 for field along c axis) (22, 29). Error bars are standard deviations. For details, we refer to the original experimental papers as cited. The Fermi liquid temperature from NMR and specific heat measurements (10) is found to be proportional to the delocalization temperature, $T_{FL} \sim 0.4 T_L$. (B) A comparison of our proposed quantum critical line (red solid line, $\alpha = 0.8$, $\eta_p = -0.025 \text{ GPa}^{-1}$) with three points on the p – H phase diagram determined from experiment (26). The result using mean field scaling behavior is shown for comparison. (B, *Inset*) A comparison of our calculated Néel temperature T_N with experiment (23, 26).

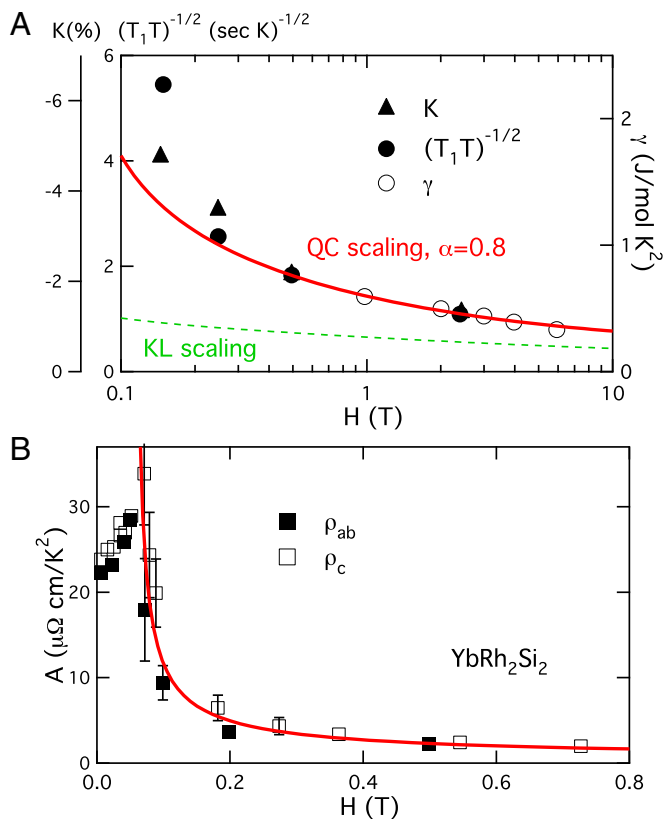


Fig. 5. The field dependence of the specific heat and magnetoresistivity coefficients for YbRh_2Si_2 . (A) A comparison with experiment of our predicted scaling for the field dependence of the specific heat, Knight shift, and spin-lattice relaxation rate (10); note that at high fields, the specific heat begins to approach the KL scaling result, Eq. 14. (B) A comparison of our proposed scaling (red solid line, $\alpha = 0.8$), Eq. 16, of the magnetoresistivity coefficients, A , with experiment (22). For the c axis resistivity, the magnetic field axis is scaled by a factor of 11. Error bars are standard deviations.

Thus, at ambient pressure its field-induced QCP at the comparatively modest field, 0.05–0.06 T, appears to mark both the end of localized behavior and long-range magnetic order, and, as may be seen in Fig. 4, that candidate QCP changes with pressure and magnetic field (26), and so represents a target of opportunity for the primarily collective framework developed in this paper. On the other hand, there are signatures of quantum critical behavior that appear to be of purely local origin, such as a line of delocalization points that change with magnetic field, but are almost unchanged by pressure (26–28), that may be ascribed to changes induced by single-ion Kondo physics.

In dealing with YbRh_2Si_2 , we first consider the delocalization line at ambient pressure and then focus our attention on understanding experiments whose results are demonstrably sensitive to both pressure and magnetic field: antiferromagnetic behavior near the QCP (10, 26), specific heat (10), resistivity (22), and spin-lattice relaxation rate (10). We will see that these quantities exhibit quantum critical scaling behavior that has a different ($\alpha = 0.8$) power law than CeCoIn_5 .

As may be seen in Fig. 4A, our model, with $T^* = 50$ K, $H_{QC} = 0.055$ T, $\eta_H = 0.07$ T $^{-1}$, and $\alpha = 0.8$, yields good agreement with experiments for the field-dependent Néel temperature (10), the delocalization line (15, 24–28), and the quantum critical line (26). The corresponding field dependence of $f_0(H)$ is plotted in Fig. 3A. We note that there have been a number of earlier proposals for T^* in the literature (2, 30, 31), but a recent photoemission experiment (31) that provides a direct measure of the onset of

coherence settled this issue, finding a $T^* = 50 \pm 10$ K, consistent with our previous estimate (2).

At ambient pressure, the delocalization line ends at the magnetic QCP and corresponds to our T_L line; it is detached from the magnetic QCP at higher pressures (26). Interestingly, we find that at high fields, the temperature that marks the onset of Landau Fermi liquid behavior, T_{FL}^p , as determined from the NMR spin-lattice relaxation rate and specific heat (10), scales with the delocalization temperature, whereas transport measurements of the cross-over to a Landau Fermi liquid regime lead to the lower values of T_{FL}^p shown there.

Importantly, our model explains the pressure dependence of the Néel temperature shown in Fig. 4B, *Inset*. On making use of Eq. 12 and assuming $T_N^0(p) = \eta_N T^*(p) = \eta_N T^*(0)(1 - \lambda p)$ with $T^*(0) = 50$ K, $\lambda = 0.1$ GPa $^{-1}$, and a frustration parameter $\eta_N = 0.21$, we find good agreement with experiment (23, 26). The nonmonotonic pressure dependence of T_N reflects the competition between the hybridization parameter $f_0(p)$, which, as it decreases with pressure, causes T_N to increase, and T^* , which, as it decreases with pressure, causes T_N to decrease. Our values of $f_0(p)$ and $T^*(p)$ for YbRh_2Si_2 are compared with those for CeCoIn_5 (16) in Fig. 3B and C; their differing pressure variations are consistent with general observations on hybridization for Ce- and Yb-based heavy electron materials.

In Fig. 5 we show that good agreement between the scaling predictions of Eq. 16 and measurements of the specific heat at 100 mK (10) and the resistivity coefficient (22) can be obtained using $\alpha = 0.8$, $\gamma_0 = 0.2$ J/mol K 2 , and $A_0 = 400$ $\mu\Omega$ cm. Interestingly, at the critical field, H_{QC} , experiment shows that the specific heat coefficient exhibits power-law scaling below 0.3 K, $\gamma(T) \propto T^{-\varepsilon}$, where $\varepsilon \approx 0.3$ –0.4 (30), in agreement with our derived scaling exponent, $\alpha/2 = 0.4$. (We note that this power-law scaling with temperature in the specific heat has apparently not yet been observed in CeCoIn_5 .)

Important additional information about quantum critical behavior in YbRh_2Si_2 comes from a two-fluid analysis of the spin-lattice relaxation rate using Eq. 17. T_1^{-1} is found to be almost constant around 50 K and modified due to crystal field effects above 80 K; on making the assumption that the local moment relaxation rate $1/T_1^{SL} = 8.5\text{s}^{-1}$ from T^* down to the lowest

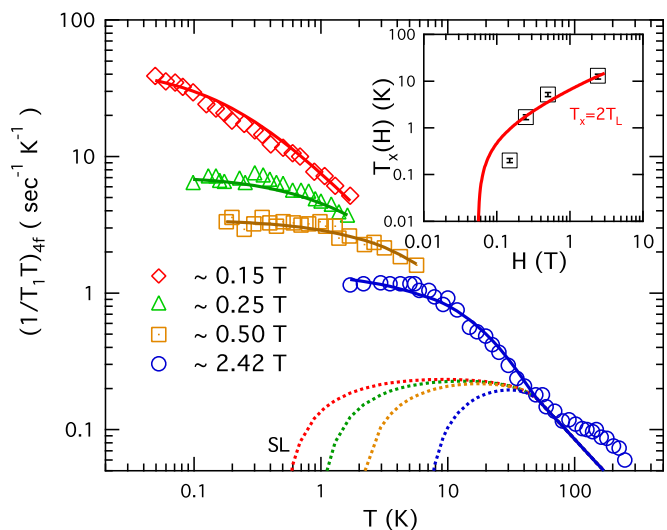


Fig. 6. A comparison with experiment of our proposed fit (solid lines, $\alpha = 0.8$) to the measured NMR spin-lattice relaxation rate in YbRh_2Si_2 (10). The dotted lines are the local moment contribution. (*Inset*) Our proposed field-dependent distance, $T_x(H) = 2T_c(H)$, of the KL spin-lattice relaxation rate from the QCP as a function of the magnetic field (solid line) is compared with the experimental points determined by isolating the KL contribution from the measured spin-lattice relaxation rate.

temperatures of interest, we can use our previously calculated values of $f(T, H)$ to obtain the local moment contribution below T^* shown in Fig. 6, and extract the KL relaxation time. It takes the form,

$$T_1^{KL} T \propto [T + T_x(H)], \quad [19]$$

As may be seen in Fig. 6, with these distinct local moment and KL components, the fit to the experimental data are remarkably good; it captures the flattening below $T_L(H)$ that in our model is due to the complete delocalization of the localized f moments described by T_L and the corresponding loss of the divergence in the local contribution.

Moreover, as may be seen in Fig. 6, *Inset*, the KL offset is given by, $T_x(H) = 2T_L(H)$. This result provides direct confirmation that the hidden magnetic quantum critical fluctuations of the KL in YbRh_2Si_2 originate in the QCP at H_{QC} , where T_1 becomes T -independent as predicted by Si et al. (32), and $T_x(H)$ represents the distance from the magnetic QCP. We further note that despite the different scaling behavior for other properties produced by their heavy electron quantum critical fluctuations, those in YbRh_2Si_2 produce the same spin-lattice relaxation behavior as those extracted for the KL in CeCoIn_5 (6). Both may originate in dynamical ω/T scaling in the KL dynamical spin-spin response function (29, 32–34).

Discussion

We have seen that the introduction of a field dependent hybridization effectiveness parameter enables us to extend our two-fluid model to the quantum critical regime and use it to explain successfully a number of different experiments involving quantum critical behavior in both CeCoIn_5 and YbRh_2Si_2 . We have been able to establish the fundamental similarities in the low frequency magnetic behavior of these materials despite their different scaling behavior near the QCP. Our ability to explain how magnetic fields change seemingly unrelated physical quantities

argues strongly that these changes originate in our proposed field-dependence of the hybridization effectiveness parameter. Importantly, we are now able to model in simple fashion the variation with magnetic field and pressure of a new and unified delocalization line, $T_L(p, H)$, that marks the loss of the partially localized behavior that leads to long-range antiferromagnetic order and provides a direct measure of distance from the QCP. Because T_L is intimately related to the determination of f_0 , its measurement yields crucial information on the evolution of the combined effects of local and collective hybridization in a large portion of the phase diagram. We have seen that T_L determines the scaling behaviors in the resistivity, specific heat, and the NMR spin-lattice relaxation rate, and that it can be determined for other materials through measurements of the Knight shift, the magnetoresistivity, and the Hall coefficient, whereas the growth of the heavy electron Fermi surface to its maximal size at T_L may be verified in future de Haas-van Alphen experiments or by photoemission spectroscopy.

Although we have shown that the phenomenological framework provided by the two-fluid model is remarkably successful in explaining the emergence of quantum critical behavior in both CeCoIn_5 and YbRh_2Si_2 , we believe it is important to continue to test it against experiments on quantum critical behavior in other heavy electron materials and to learn from experiment whether α may change across the QCP and whether there are materials in which quantum critical scaling gives rise to a power-law dependence in $(p - p_c^0)$.

ACKNOWLEDGMENTS. Y.-f.Y. thanks Frank Steglich for helpful discussions and calling the authors' attention to the magnetostriction experiment in YbRh_2Si_2 . Y.-f.Y. and D.P. thank Elihu Abrahams for helpful comments on the manuscript, and the Aspen Center for Physics (National Science Foundation Grant 1066293) and the Santa Fe Institute for their hospitality during the writing of this paper. Y.-f.Y. is supported by the National Natural Science Foundation of China (Grant 11174339) and the Strategic Priority Research Program of the Chinese Academy of Sciences (Grant XDB07000000).

- Yang Y-F, Pines D (2012) Emergent states in heavy-electron materials. *Proc Natl Acad Sci USA* 109(45):E3060–E3066.
- Yang Y-F, Fisk Z, Lee H-O, Thompson JD, Pines D (2008) Scaling the Kondo lattice. *Nature* 454(7204):611–613.
- Nakatsuji S, Pines D, Fisk Z (2004) Two fluid description of the Kondo lattice. *Phys Rev Lett* 92(1):016401.
- Curro NJ, Young B-L, Schmalian J, Pines D (2004) Scaling in the emergent behavior of heavy-electron materials. *Phys Rev B* 70(23):235117.
- Yang Y-F, Pines D (2008) Universal behavior in heavy-electron materials. *Phys Rev Lett* 100(9):096404.
- Yang Y-F, Urbano RR, Curro NJ, Pines D, Bauer ED (2009) Magnetic excitations in the kondo liquid: Superconductivity and hidden magnetic quantum critical fluctuations. *Phys Rev Lett* 103(19):197004.
- Shirer KR, et al. (2012) Long range order and two-fluid behavior in heavy electron materials. *Proc Natl Acad Sci USA* 109(45):E3067–E3073.
- Laughlin RB, Lonzarich GG, Monthoux P, Pines D (2001) The quantum criticality conundrum. *Adv Phys* 50(4):361–365.
- Sachdev S (1999) *Quantum Phase Transitions* (Cambridge Univ Press, Cambridge, UK).
- Ishida K, et al. (2002) YbRh_2Si_2 : Spin fluctuations in the vicinity of a quantum critical point at low magnetic field. *Phys Rev Lett* 89(10):107202.
- Ronning F, et al. (2006) Pressure study of quantum criticality in CeCoIn_5 . *Phys Rev B* 73(6):064519.
- Zaum S, et al. (2011) Towards the identification of a quantum critical line in the (p, B) phase diagram of CeCoIn_5 with thermal-expansion measurements. *Phys Rev Lett* 106(8):087003.
- Urbano RR, et al. (2007) Interacting antiferromagnetic droplets in quantum critical CeCoIn_5 . *Phys Rev Lett* 99(14):146402.
- Yang Y-F (2013) Anomalous Hall effect in heavy electron materials. *Phys Rev B* 87(4):045102.
- Paschen S, et al. (2004) Hall-effect evolution across a heavy-fermion quantum critical point. *Nature* 432(7019):881–885.
- Nicklas M, et al. (2001) Response of the heavy-fermion superconductor CeCoIn_5 to pressure: Roles of dimensionality and proximity to a quantum-critical point. *J Phys Condens Matter* 13(44):L905–L912.
- Kim JS, Alwood J, Stewart GR, Sarrao JL, Thompson JD (2001) Specific heat in high magnetic fields and non-Fermi-liquid behavior in CeMIn_5 ($M=\text{Ir, Co}$). *Phys Rev B* 64(13):134524.
- Sidorov VA, et al. (2002) Superconductivity and quantum criticality in CeCoIn_5 . *Phys Rev Lett* 89(15):157004.
- Paglione J, et al. (2003) Field-induced quantum critical point in CeCoIn_5 . *Phys Rev Lett* 91(24):246405.
- Singh S, et al. (2007) Probing the quantum critical behavior of CeCoIn_5 via Hall effect measurements. *Phys Rev Lett* 98(5):057001.
- Kohori Y, et al. (2006) ^{115}In NQR studies of CeRhIn_5 and CeCoIn_5 under high pressure. *J Alloy Comp* 408–412:51–53.
- Gegenwart P, et al. (2002) Magnetic-field induced quantum critical point in YbRh_2Si_2 . *Phys Rev Lett* 89(5):056402.
- Knebel G, et al. (2005) High-pressure phase diagram of YbRh_2Si_2 . *Phys B* 359–361:20–22.
- Gegenwart P, et al. (2006) High-field phase diagram of the heavy-fermion metal YbRh_2Si_2 . *New J Phys* 8(9):1–12.
- Gegenwart P, et al. (2007) Multiple energy scales at a quantum critical point. *Science* 315(5814):969–971.
- Tokiwa Y, Gegenwart P, Geibel C, Steglich F (2009) Separation of energy scales in undoped YbRh_2Si_2 under hydrostatic pressure. *J Phys Soc Jpn* 78(12):123708.
- Friedemann S, et al. (2009) Detaching the antiferromagnetic quantum critical point from the Fermi-surface reconstruction in YbRh_2Si_2 (2009). *Nat Phys* 5(7):465–469.
- Friedemann S, et al. (2010) Magnetic and electronic quantum criticality in YbRh_2Si_2 . *J Low Temp Phys* 161(1-2):67–82.
- Pfau H, et al. (2012) Thermal and electrical transport across a magnetic quantum critical point. *Nature* 484(7395):493–497.
- Steglich F, et al. (2013) Evidence for a Kondo destroying quantum critical point in YbRh_2Si_2 . arXiv:1309.7260.
- Mo S-K, et al. (2012) Emerging coherence with unified energy, temperature, and lifetime scale in heavy fermion YbRh_2Si_2 . *Phys Rev B Rapid Commun* 85(24):241103.
- Si Q, Rabello S, Ingersent K, Smith JL (2001) Locally critical quantum phase transitions in strongly correlated metals. *Nature* 413(6858):804–808.
- Wölfle P, Abrahams E (2011) Quasiparticles beyond the Fermi liquid and heavy fermion criticality. *Phys Rev B Rapid Commun* 84(4):041101.
- Abrahams E, Wölfle P (2012) Critical quasiparticle theory applied to heavy fermion metals near an antiferromagnetic quantum phase transition. *Proc Natl Acad Sci USA* 109(9):3238–3242.